Predicting postoperative delirium assessed by the Nursing Screening Delirium Scale in the recovery room for non-cardiac surgeries without craniotomy: A retrospective study using a machine learning approach

Niklas Giesa[1], Stefan Haufe[1,2,3], Mario Menk[1], Björn Weiß[1], Claudia Spies[1], Sophie K. Piper[1], Felix Balzer[1,*], Sebastian D. Boie[1,*]

niklas.giesa@charite.de
[1]Charité – Universitätmedizin Berlin, 10117, Berlin, Germany
[2]Technische Universität Berlin, 10623, Berlin, Germany
[3]Physikalisch Technische Bundesanstalt, 10587, Berlin, Germany

Abstract

Background: Postoperative delirium (POD) contributes to severe outcomes such as death or development of dementia. Thus, it is desirable to identify vulnerable patients in advance during the perioperative phase. Previous studies mainly investigated risk factors for delirium during hospitalization and further used a linear logistic regression (LR) approach with time-invariant data. Studies have not investigated patients' fluctuating conditions to support POD precautions.
Objective: In this single-center study, we aimed to predict POD in a recovery room setting with a non-linear machine learning (ML) technique using pre-, intra-, and postoperative data.
Methods: The target variable POD was defined with the Nursing Screening Delirium Scale (Nu-DESC) ≥ 1. Feature selection was conducted based on robust univariate test statistics and L_1 regularization. Non-linear multi-layer perceptron (MLP) as well as tree-based models were trained and evaluated – with the receiver operating characteristics curve (AUROC), the area under precision recall curve (AUPRC), and additional metrics – against LR and published models on bootstrapped testing data.
Results: The prevalence of POD was 8.2% in a sample of 73,181 surgeries performed between 2017 and 2020. Significant univariate impact factors were the preoperative ASA status, the intraoperative amount of given remifentanil, and the postoperative Aldrete score. The best model used pre-, intra-, and postoperative data. The tree-based model achieved a mean AUROC of 0.854 and a mean AUPRC of 0.418 outperforming linear LR, well as best applied and retrained baseline models.
Conclusions: Overall, non-linear machine learning models using data from multiple perioperative time phases were superior to traditional ones in predicting POD in the recovery room. Class imbalance was seen as a main impediment for model application in clinical practice.
Keywords: Postoperative delirium; recovery room; machine learning; multi-layer perceptron, prediction models

Author Summary

Currently, the pathophysiology of postoperative delirium (POD) is unknown. Hence, there is no dedicated medication for treatment. Patients who experience POD are oftentimes mentally disturbed causing pressure on related family members, clinicians, and the health system. With our study, we want to detect POD before onset trying to give decision support to health professionals. Vulnerable patients could be transferred to delirium wards mitigating the risk of severe outcomes such as permanent cognitive decline. We also provide insides into clinical parameters - recorded before, during, and after the surgery - that could be adapted for reducing POD risk. Our work is openly available, developed for clinical implementation, and could be transferred to other clinical institutions.

Introduction

Postoperative delirium (POD) as an acute state of brain dysfunction after a surgery has been found to be related to adverse long-term effects – such as increased length of hospitalization, development of dementia, and death [1-3]. Reported incidences (3-50%) vary substantially depending on the cohort definition and are elevated in major surgical cases as well as in elderly patients [4-7]. Recent studies stress the need for an early assessment of POD onset in the recovery room enabling clinicians to improve patients' outcomes [2, 4, 8]. Assessment scores for a recovery room setting which are validated against DSM-5 criteria comprise the Confusion Assessment Method (CAM) and the Nursing Screening Delirium Scale (Nu-DESC) [8-10]. In contrast to the CAM, the Nu-DESC is a purely observational score that has been validated to have a sensitivity of up to 80% for scores ≥ 1 [8, 10].

Due to the high relevance in perioperative care, previous POD studies were not limited to finding predisposing factors – such as comorbidity or age – and precipitating factors – such as surgical complications or intraoperative blood loss [2, 8, 11, 12]. Studies went further by applying multivariable prediction models. Most of them evaluated the delirium onset during hospitalization with the CAM and used a linear logistic regression (LR) technique [13-17]. Popular models by Boogaard et al. and Wassenaar et al. show good test performance as measured by the area under the receiver operating characteristics curve (AUROC=0.75-0.89) [18-20] but diminished performance on external data (AUROC=0.62) [21]. A few authors trained non-linear machine learning algorithms predicting POD [4, 22, 23, 24]. Xu et al. used ICD-9 encoded POD as a target variable for a deep multi-layer perceptron (MLP) architecture. Using pre- and intraoperative variables extracted from 111,888 electronic health records (EHRs) as features, the authors achieved an AUROC of 0.72 [22]. Although Xu et al. capture the fluctuating physiology in the intraoperative phase, a meta-study by Ruppert et al. highlights that most of the published prediction models use values from a single point in time [25].

Our aim was to identify patients vulnerable to suffering from POD in the recovery room. Pre-, intra-, and postoperative variables were extracted from EHRs and combined into different prognostic non-linear models. We used the Nu-DESC in a recovery room setting for defining POD. An automated risk assessment after the end

of the surgery could help transferring vulnerable patients to specialized noise-reduced wards improving their outcome [8, 26, 27].

Methods

Ethics Statement

This study was performed under ethics approval granted by the independent ethics committee at Charité – Universitätsmedizin Berlin (vote EA4/254/21). We performed analysis on pseudonymous data. Data processing consent was obtained by a formal in-hospital treatment contract.

Cohort and Target Variable

EHRs were extracted for admissions between 01/01/2017 and 12/31/2020. Patients who underwent cardiovascular or craniotomy procedures were excluded due to the increased risk of postoperative complications [5, 14, 17, 28]. All other adult patients (≥ 18 years) who were assessed with at least one Nu-DESC in the recovery room were included. The POD positive (y=1) group consisted of surgeries on patients who were evaluated with at least one Nu-DESC score ≥ 1 in the recovery room [8]. If all Nu-DESC scores in the recovery room were equal to 0, the surgery was assigned to the negative group (y=0).

Figure 1: Cohort definition based on inclusion criteria. Number of patients, - hospital stays and - surgeries are provided at each step. A positive target variable y=1 was defined based on the presence of at least one Nu-DESC score ≥ 1. A negative y=0 was defined if all Nu-DESC scores were equal to 0.

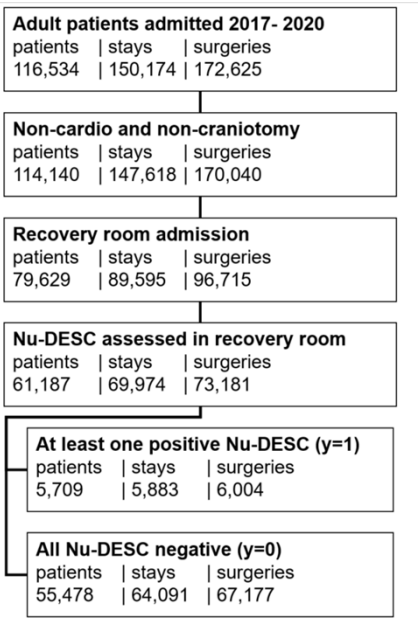

Table 1: Baseline characteristics for all patients in the POD positive (y=1) and negative (y=0) groups. The mean, [1st, 2nd, 3rd] quartiles are shown for numerical values, counts are displayed otherwise. The type of surgery is defined using clinical codes described in Extended Table 2 in Appendix 1.

		Unit	All	POD Positives (y=1)	POD Negatives (y=0)
Counts					
	Patients	-	61,187	5,709	55,478
	Stays	-	69,974	5,883	64,091
	Surgeries	-	73,181	6,004	67,177
	Surgeries per stay	-	1.15, [1, 1, 1]	1.15, [1, 1, 1]	1.14, [1, 1, 1]
	Previous admissions	-	0.90, [0, 0, 1]	1.00, [0, 0, 1]	0.80, [0, 0, 1]
	Previous surgeries per stay	-	0.51, [0, 0, 1]	0.53, [0, 0, 1]	0.49, [0, 0, 1]
Demographics					
	Age	years	56, [42, 60, 73]	60, [46, 62, 76]	52, [36, 53, 67]
	Gender	-	28,013 male (46%) 33,174 female (54%)	2,927 male (51%) 2,782 female (49%)	25,086 male (47%) 30,392 female (53%)
	BMI	kg/m^2	26.91, [22.80, 25.70, 29.47]	26.91, [22.85, 25.76, 29.38]	26.91, [22.75, 25.64, 29.57]
	ASA status	-	2.07, [2, 2, 3]	2.37, [2, 2, 3]	2.04, [2, 2, 3]
	OP N urgency class	-	4.00, [3, 5, 5]	3.89, [3, 5, 5]	4.02, [3, 5, 5]
Hospitalization					
	Length of hospital stay	days	8.66, [3.25, 5.09, 9.05]	10.53, [3.08, 6.00, 11.00]	6.80, [2.22, 3.78, 7.09]
	Length of anesthesia	hours	2.22, [1.14, 1.69, 2.54]	2.44, [1.45, 2.14, 3.06]	1.99, [1.12, 1.65, 2.49]
	Length of surgery	hours	1.28, [0.48, 0.86, 1.50]	1.43, [0.63, 1.13, 1.88]	1.14, [0.47, 0.84, 1.46]
	Length of recovery room stay	hours	2.51, [1.08, 1.59, 2.32]	2.92, [1.45, 2.08, 3.01]	2.11, [1.05, 1.54, 2.24]
Nu-DESC evaluation					
	Number of Nu-DESC evaluations	-	1.09, [1, 1, 1]	1.12, [1, 1, 1]	1.09, [1, 1, 1]
	Duration between recovery room admission and 1st Nu-DESC evaluation	minutes	50.52, [7.79, 32.03, 69.22]	35.55, [4.03, 10.84, 38.99]	51.83, [8.67, 34.26, 71.05]
	Duration between last Nu-DESC evaluation and recovery room discharge	minutes	75.02, [17.97, 40.12, 80,54]	133.33, [50.46, 93.34, 144.25]	69.90, [17.00, 37.19, 74.15]
Type of surgery					
	Locomotive organs	-	20,369 (37%)	2,293 (38%)	18,103 (27%)
	Organs of the head	-	12,680 (19%)	743 (12%)	11,937 (18%)
	Nervous system	-	8,205 (12%)	1,034 (17%)	7,171 (11%)
	Digestive tract	-	8,674 (13%)	764 (12%)	7,910 (13%)
	Skin and tissue	-	7,580 (11%)	890 (15%)	6,690 (11%)
	Urinary system	-	6,381 (10%)	597 (9%)	5,784 (9%)
	Blood vessels	-	3,061 (5%)	344 (6%)	2,717 (4%)
	Respiratory tract	-	3,705 (6%)	395 (7%)	3,310 (5%)
	Hormone system	-	807 (1%)	114 (2%)	693 (1%)
Type of anesthesia					
	General balanced	-	36,730 (50%)	2,819 (47%)	33,911 (50%)
	Total intravenous	-	31,720 (43%)	3,255 (54%)	28,465 (42%)
	Epidural	-	2,639 (3%)	131 (2%)	2,508 (4%)
	Spinal	-	3,776 (5%)	49 (1%)	3,727 (6%)
	Analgo	-	1,145 (1%)	91 (2%)	1,054 (2%)
	Other	-	3,405 (4%)	258 (4%)	3,147 (5%)

Figure 1 summarizes the inclusion criteria yielding the cohort of 61,187 patients with 69,974 hospital stays and 73,181 performed surgeries. POD incidence was 9.3%, 8.4% and 8.2% for distinct patients, hospital stays and surgeries respectively.

Table 1 displays baseline characteristics for the selected cohort. Additional characteristics are shown in Extended Table 1, 2, and in Extended Figure 1 in Appendix 2.

Perioperative Time Phases

The hospital stays were divided into three distinct perioperative time phases. Data from the preoperative (T1) -, intraoperative (T2) -, and postoperative (T3) phase as well as time-invariant (TI) data were considered rather than focusing on one value from a single point in time. Figure 2 highlights the start - and end events for T1-T3.

Figure 2: Hospitalization schema with relevant intraoperative points in time. Definition of time phases T1-T3 are based on highlighted events. TI holds time-invariant data and is not included in the graphic. When multiple Nu-DESC evaluations were performed in the recovery room, the timestamp of the first one was chosen for phases including T3.

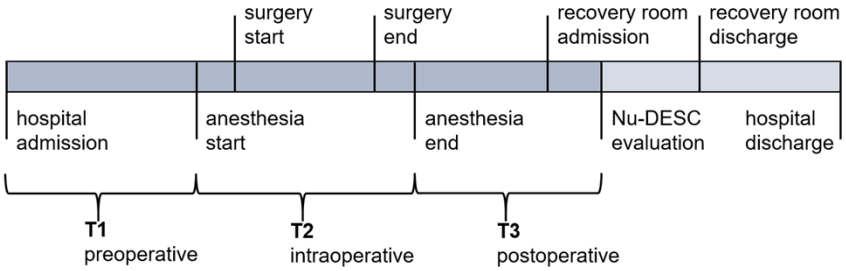

For the POD prediction task, distinct time phases (T1-T3) were considered individually or combined. A different model (M1-M123) was trained and evaluated for each combination with data from assigned time phases (see Table 2). In the following, time phases and their combinations are named as T1-T123, data from TI is always included.

Table 2: Models which are fed with data from corresponding time phase combinations. The start (from) and end (to) of each combination is introduced as well. TI data is included for all models.

Model	Time Phases	From	To
M1	T1	hospital admission	anesthesia start
M2	T2	anesthesia start	anesthesia end
M3	T3	anesthesia end	1st Nu-DESC evaluation in the recovery room
M12	T12 (T1+T2)	hospital admission	anesthesia end
M23	T23 (T2+T3)	anesthesia start	1st Nu-DESC evaluation in the recovery room
M123	T123 (T1+T2+T3)	hospital admission	1st Nu-DESC evaluation in the recovery room

Feature Extraction and Preprocessing

Data were extracted from the clinical information systems (CIS) of three sides at our clinical center. Based on literature review and clinical expertise [11-25], a total of 549 clinical variables – including 253 categorical and 296 numerical ones – were

identified with respect to T1-T3 and TI. Extended Table 3 in Appendix 2 shows the number of extracted variables per time phase and clinical domain.

EHRs might suffer from integrity issues due to distributed CIS [29, 30]. Thus, extraction scripts were refined until there were no discrepancies with the front-end for a sample of 50 surgeries. For numerical variables, valid thresholds (lower and upper bounds) were applied to remove impossible values (e.g., negative oxygen saturation) (see Extended Table 1 in Appendix 1). Extended Table 4 in Appendix 2 outlines further details about feature encodings.

Univariate Test Statistics

Robust Mann-Whitney U (MWU) tests [31] were used to evaluate the discriminatory power of numerical parameters with respect to the POD target. False discovery rate (FDR) correction [32] with alpha=0.05 was applied to identify statistically significant variables. The AUROC – which can be derived from the MWU statistic [33] – was used to quantify effect-sizes. AUROC values are normalized between 0 and 1, where 1 indicates a perfect positive association, 0 indicates a perfect negative association, and 0.5 indicates chance-level discrimination. The absolute strength of an effect – regardless of the direction – was calculated for each significant variable as $e=2|\text{AUROC}-0.5|$. For categorical variables, we used the odds ratio (OR) of a univariate logistic regression [34] as a measure of effect size. A direction independent measure of effect size was defined as $o=|\log(\text{OR})|$. We have performed feature selection processes based on univariate tests and based on a L_1-norm regularization. The concrete implementation is described in Appendix 2 under Feature Selection.

Data Splitting, Cross-Validation and Standardization

The extracted data were initially split (80/20%) into train – and test sets. To avoid dependencies between these sets we used patient identifiers to perform the splitting. Stratification with the target variable was done so that the incidence of POD was preserved in both sets. As a result, the testing set comprised 12,238 patients, the training set included 48,949 patients.

The training data were used to evaluate models with different feature sets and hyperparameters. A 3-fold cross validation (CV) technique [35] was applied where a configuration was determined from 66.6% and evaluated on 33.3% of the training data. This evaluation was iteratively performed three times. For each model variant (M1-M123), each feature set was used in a hyperparameter search. The best performing configuration across all CV iterations per feature set was chosen on basis of the lowest validation loss for the final evaluation on the test set. Numerical features were standardized using z-transformation [36]. Feature mean values as well as standard deviations were calculated on the training data, applied to validation – and eventually to the test data. Extracted training set mean values were also used to impute missing values in train, validation, and test sets.

Machine Learning Techniques and Hyperparameter Search

Two types of non-linear models were trained in comparison to linear-, and baseline models. First, deep multi-layer perceptrons (MLPs) [37-39] were trained to predict POD. Extended Table 5 in Appendix 2 outlines the ranges of values optimized with Grid - [40] or Random Search [41] for a fully connected MLP architecture. We used focal loss [42] or weighted binary cross-entropy (BCE) [43] since they have been shown to be able to deal with unbalanced classification problems such as ours. L_1-norm regularization [44] was applied on the first layer of the MLP when using all available features instead of feature subsets. Extended Table 6 in Appendix 2 displays results from the CV process.

In addition to MLPs, we included two non-linear ensemble machine learning approaches based on decision trees. Random forest and gradient boosting classifier were integrated into Random Search [45, 46]. Extended Table 7 in Appendix 2 outlines the parameter search space for tree-based models. Weighted BCE was configured for both algorithms. Appendix 2 displays results from the CV process with tree-based models.

We further compared the highly non-linear architectures with a linear logistic regression (LR) using a weighted BCE. LR models incorporated all available features per corresponding time phase (T1-T123). Constructed models (M1-M123) were also compared to LR models by Wassenaar and Boogaard [18-20]. The authors predicted delirium onset during an intensive care unit (ICU) stay assessed with the CAM. Due to the simplicity and open accessibility, we applied pre-trained models on data from time phase combinations (T1-T123). Models by Wassenaar and Boogaard were retrained and evaluated with a LR, a MLP and boosted tree technique.

The performance of the obtained predictions was assessed by means of either the AUROC or the area under the precision recall curve (AUPRC) [47, 48]. The AUROC is less suitable - biased towards large values - for highly imbalanced classification problems such as ours. This problem is less pronounced for the AUPRC [48, 49], which focuses the minority class. Additionally, the F1-score was computed [50]. To estimate standard errors of the mean model performances, bootstrapping – random sampling with replacement – was applied 1000 times on the test data [51].

Code Availability and Reporting

The code including trained models, preprocessing scripts, usage notes, and descriptions are openly accessible [52]. The data has not been published due to German data protection regulations. Results are reported in accordance with the TRIPOD guidelines (see Extended Table 6 in Appendix 2) [53].

Results

Perioperative Variables

Table 3: Ten most discriminative numerical variables per time phase sorted by effect size defined as e=2|AUROC-0.5| and calculated via univariate Mann-Whitney U tests on the training set. The effect direction is indicated by (+)/ (−). *P*-values are FDR corrected with alpha=0.05. Significant variables are included solely (all *P*-values <.001). Missing rates are reported as fraction of patients having values for a given variable from all patients. For time-resolved measurements, performance of aggregate scores is reported, where the 10th, 50th, and 90th percentiles are denoted as p10, p50, and p90, the median absolute deviation is denoted as map, and the sum across time is denoted as sum. Time invariant (TI), preoperative (T1), intraoperative (T2) and postoperative (T3) variables are included.

	Variable	2|AUROC-0.5|	AUC	Missing rate
TI				
	Age	(+) 0.232	0.616	0.000
	Number of previous diagnoses	(+) 0.134	0.566	0.000
	History of psychiatric disorder	(+) 0.121	0.560	0.000
	History of unspecific delirium	(+) 0.073	0.536	0.000
	History of hypertension	(+) 0.068	0.533	0.000
	Number of previous admissions	(+) 0.068	0.533	0.000
	Body length	(−) 0.051	0.474	0.547
	History of dementia	(+) 0.043	0.521	0.000
	History of respiratory failure	(+) 0.043	0.521	0.000
	History of diabetes mellitus	(+) 0.040	0.519	0.000
T1				
	ASA status p90	(+) 0.179	0.589	0.476
	Metabolic equivalents p50	(−) 0.178	0.410	0.866
	SpO2 p10	(−) 0.155	0.422	0.360
	Hematocrit in blood p90	(−) 0.140	0.430	0.891
	Calcium in blood p10	(−) 0.139	0.430	0.890
	Hospitalization duration	(+) 0.129	0.564	0.000
	Erythrocytes in blood p10	(-) 0.116	0.442	0.436
	Hemoglobin in blood p0.1	(-) 0.108	0.446	0.431
	Ppeak p90	(+) 0.100	0.550	0.844
	BP systolic	(+) 0.082	0.541	0.497
T2				
	Anesthesia duration	(+) 0.218	0.609	0.000
	Amount remifentanil p50	(+) 0.200	0.600	0.695
	Surgery duration	(+) 0.183	0.591	0.000
	Amount remifentanil sum	(+) 0.178	0.588	0.695
	SEF right p50	(−) 0.175	0.412	0.807
	SEF left p10	(−) 0.173	0.414	0.807
	PCV ventilation therapy duration	(+) 0.166	0.582	0.000
	Endotracheal tube access duration	(+) 0.152	0.575	0.000
	Hospitalization duration	(+) 0.146	0.573	0.000
	BP systolic p90	(+) 0.143	0.571	0.217
T3				
	Aldrete score p90	(−) 0.347	0.327	0.079
	Recovery room duration	(−) 0.232	0.384	0.000
	Anesthesia duration	(+) 0.219	0.609	0.000
	Surgery duration	(+) 0.183	0.591	0.000
	Respiratory rate p10	(+) 0.179	0.589	0.745
	PCV ventilation therapy duration	(+) 0.161	0.580	0.000
	Endotracheal tube access duration	(+) 0.151	0.575	0.000
	Heart rate p10	(+) 0.144	0.572	0.233
	Respiratory rate p50	(+) 0.143	0.571	0.745
	Pulse map	(−) 0.139	0.431	0.518

Table 4: Top 5 most discriminative categorical variables per time phase, sorted by effect size. The effect size is defined as |log(OR)| and calculated on the training set using univariate linear logistic regression. The effect direction is indicated by (+)/ (–). Time invariant (TI), preoperative (T1), intraoperative (T2) and postoperative (T3) variables are included. The OR 95% confidence interval (CI) serves as an uncertainty estimate.

	Variable	|log(OR)|	OR	95% CI
TI				
	OPS history nervous system	(+) 0.86	2.35	[1.95, 2.82]
	OPS nervous system	(+) 0.82	2.26	[1.93, 2.63]
	OPS hormone system	(+) 0.75	2.11	[1.64, 2.70]
	OPS history hormone system	(+) 0.67	1.96	[1.46, 2.61]
	OPS visual organs	(–) 0.62	0.54	[0.35, 0.81]
T1				
	Type spinal anesthesia	(–) 2.63	0.07	[0.02, 0.22]
	Dementia	(+) 2.48	11.92	[8.21, 17.3]
	Dissociative disorder	(+) 2.01	7.45	[1.24, 44.60]
	Cognitive impairment	(+) 1.68	5.39	[2.77, 10.45]
	Parkinson disease	(+) 1.45	4.28	[3.22, 5.69]
T2				
	Dementia	(+) 3.33	27.96	[5.42, 144.15]
	Urine drain access complication	(+) 2.82	16.77	[2.80, 100.38]
	Amputation	(+) 2.70	14.91	[3.33, 66.63]
	Drug related disorder	(+) 2.01	7.45	[1.24, 44.60]
	Peripheral vascular disease	(+) 1.96	7.12	[2.75, 18.37]
T3				
	Dementia	(+) 3.11	22.36	[4.09, 122.12]
	General op complication	(+) 2.41	11.18	[2.25, 55.40]
	Drug class benzodiazepine	(+) 1.53	4.61	[2.47, 8.59]
	Peripheral arterial disease	(+) 1.01	2.74	[1.45, 5.15]
	Parkinson disease	(+) 0.98	2.68	[1.42, 5.04]

Univariate correlations between individual numerical as well as categorical variables and the POD target are presented in Table 3 and
Table 4. Highly correlated clinical variables were age (e=0.232, with e=2|AUROC-0.5|) for TI, the ASA status (e=0.179) for T1, the intraoperative (T2) amount of remifentanil (e=0.200), and the Aldrete score (e=0.347) measured in the recovery room (T3). The anesthesia-, and the surgery durations calculated for each timeline are highly discriminative in both, the intraoperative - (T2) and the postoperative (T3) phase. In some cases, variables with relatively high effect size had high missing rate – like the 50th percentile of the right intraoperative spectral edge frequency (SEF) (e=0.175, 0.807 missing rate).

As seen in
Table 4, dementia is the categorical variable with the highest positive association with POD encoded as EHR for all three timelines T1-T3 (o=2.48, o=2.48, o=3.33). Uncertainty according to the 95% confidence interval (CI) calculated with the odds ratio [69] was very high for this variable. OPS surgical procedure history regarding the nervous system (o=0.86), the absent application of spinal anesthesia (o=2.63), urine drain access complication (o=2.82) as well as general op complication (o=2.41) are strong discriminative factors within TI, TL1-TL3 respectively.

Model Evaluation

Figure 3: POD classification performance of different models according to the area under the receiver operating characteristics curve (AUROC), and the area under the precision-recall curve (AUPRC) calculated on the test set. Metrics are evaluated either for the MLP or tree model per variant (M1-M123, corresponding to time phases T1-T123, upper graphs) or per machine learning model class applied only to the intraoperative phase (T12, lower graphs). Every model variant includes time-invariant data (TI). Referenced baseline models are indicated by 1st author's name – Wassenaar or Boogaard - as prefix, recalibrated models are indicated as rec. Baseline models were either pre-trained (pretr), retrained using logistic regression - (lr) or retrained using a multi-layer perceptron (mlp).

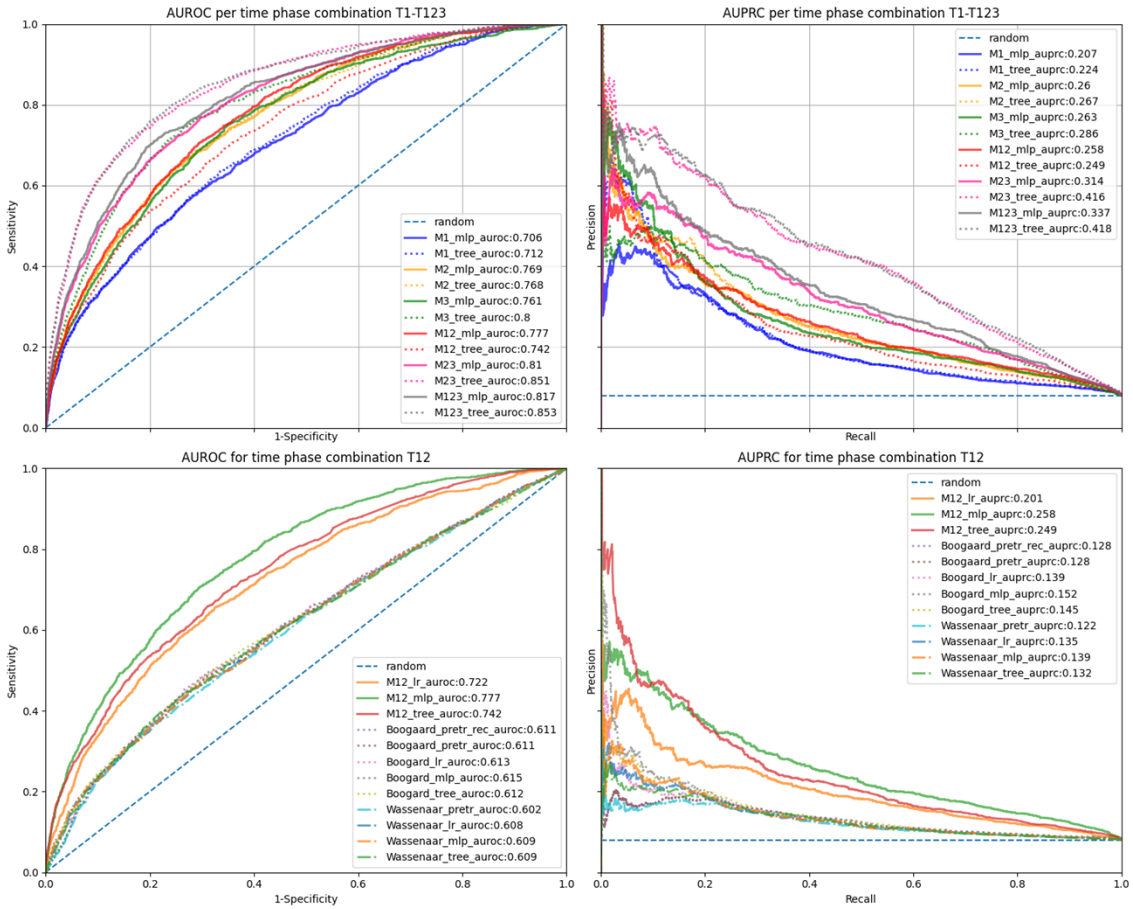

Table 5: Performance metrics (mean, [95% confidence interval]) on bootstrapped test sets for trained logistic regression (lr), multi-layer-perceptron (mlp), tree-based models (tree), or pre-trained (pretr) models. The best baseline models according to the AUROC and AUPRC metrics (Wassenaar and Boogaard) are also included. Sensitivity and specificity are calculated for the threshold that maximizes their sum. Precision is calculated for the highest threshold for which recall > 0.70. Model variants (M1-M123) consume data from time phases and their combinations T1-T123. Data from TI is included for every model.

	Model	AUROC	AUPRC	Sensitivity	Specificity	Precision	F1-Score
T1							
	M1_lr	0.698, [0.697, 0.699]	0.181, [0.180, 0.182]	0.615, [0.609, 0.621]	0.677, [0.670, 0.683]	0.125, [0.124, 0.125]	0.231, [0.230, 0.233]
	M1_mlp	0.708, [0.706, 0.709]	0.206, [0.205, 0.207]	0.582, [0.574, 0.589]	0.713, [0.706, 0.720]	0.126, [0.125, 0.127]	0.239, [0.238, 0.241]
	M1_tree	0.715, [0.714, 0.716]	0.224, [0.223, 0.226]	0.618 [0.612, 0.624]	0.691, [0.684, 0.697]	0.128, [0.127, 0.128]	0.240, [0.238, 0.241]
	Boogard_mlp	0.610, [0.610, 0.611]	0.146, [0.145, 0.146]	0.438, [0.437, 0.439]	0.740, [0.740, 0.741]	0.098, [0.098, 0.098]	0.203, [0.201, 0.203]

	Wassenaar_mlp	0.610, [0.609, 0.611]	0.139, [0.138, 0.141]	0.452, [0.451, 0.453]	0.722, [0.721, 0.723]	0.097, [0.096, 0.098]	0.198, [0.198, 0.199]
T2							
	M2_lr	0.711, [0.710, 0.712]	0.183, [0.182, 0.184]	0.662, [0.656, 0.668]	0.658, [0.653, 0.664]	0.135, [0.134, 0.136]	0.237, [0.236, 0.239]
	M2_mlp	0.766, [0.766, 0.767]	0.253, [0.252, 0.255]	0.742, [0.737, 0.747]	0.649, [0.644, 0.655]	0.161, [0.160, 0.161]	0.258, [0.256, 0.259]
	M2_tree	0.771, [0.770, 0.772]	0.273, [0.272, 0.275]	0.732, [0.728, 0.736]	0.676, [0.672, 0.681]	0.167, [0.167, 0.168]	0.269, [0.268, 0.270]
	Boogard_mlp	0.609, [0.608, 0.611]	0.146, [0.145, 0.147]	0.450, [0.446, 0.454]	0.728, [0.724, 0.732]	0.098, [0.098, 0.099]	0.202, [0.201, 0.203]
	Wassenaar_mlp	0.609, [0.608, 0.610]	0.139, [0.138, 0.140]	0.459, [0.452, 0.467]	0.716, [0.709, 0.723]	0.097, [0.097, 0.098]	0.198, [0.197, 0.199]
T3							
	M3_lr	0.768, [0.767, 0.769]	0.238, [0.237, 0.239]	0.692, [0.688, 0.697]	0.715, [0.710, 0.719]	0.169, [0.167, 0.170]	0.279, [0.278, 0.280]
	M3_mlp	0.763, [0.762, 0.764]	0.254, [0.252, 0.255]	0.784, [0.782, 0.786]	0.629, [0.627, 0.631]	0.163, [0.163, 0.164]	0.259, [0.259, 0.260]
	M3_tree	0.799, [0.799, 0.800]	0.285, [0.284, 0.287]	0.740, [0.737, 0.743]	0.741, [0.738, 0.744]	0.211, [0.210, 0.212]	0.315, [0.313, 0.316]
	Boogard_mlp	0.606, [0.605, 0.607]	0.137, [0.136, 0.138]	0.449, [0.445, 0.454]	0.723, [0.719, 0.728]	0.097, [0.096, 0.097]	0.197, [0.196, 0.198]
	Wassenaar_mlp	0.609, [0.608, 0.61]	0.135, [0.134, 0.136]	0.442, [0.436, 0.448]	0.736, [0.731, 0.741]	0.098, [0.097, 0.098]	0.201, [0.20, 0.202]
T12							
	M12_lr	0.722, [0.721, 0.723]	0.201, [0.200, 0.202]	0.639, [0.633, 0.644]	0.695, [0.691, 0.700]	0.137, [0.136, 0.138]	0.249, [0.248, 0.251]
	M12_mlp	0.777, [0.776, 0.778]	0.269, [0.268, 0.271]	0.760, [0.752, 0.767]	0.652, [0.644, 0.659]	0.167, [0.167, 0.168]	0.265, [0.263, 0.267]
	M12_tree	0.740, [0.739, 0.741]	0.246, [0.244, 0.247]	0.651, [0.644, 0.659]	0.696, [0.689, 0.704]	0.142, [0.141, 0.143]	0.255, [0.253, 0.256]
	Boogard_tree	0.613, [0.612, 0.613]	0.139, [0.138, 0.139]	0.486, [0.485, 0.487]	0.698, [0.697, 0.699]	0.101, [0.100, 0.102]	0.202, [0.201, 0.203]
	Wassenaar_mlp	0.609, [0.608, 0.609]	0.151, [0.15, 0.152]	0.663, [0.659, 0.667]	0.598, [0.594, 0.601]	0.121, [0.121, 0.122]	0.214, [0.214, 0.215]
T23							
	M23_lr	0.751, [0.750, 0.752]	0.227, [0.226, 0.229]	0.708, [0.703, 0.713]	0.676, [0.672, 0.681]	0.159, [0.159, 0.160]	0.262, [0.260, 0.263]
	M23_mlp	0.816, [0.815, 0.817]	0.341, [0.339, 0.342]	0.767, [0.764, 0.770]	0.728, [0.726, 0.730]	0.216, [0.214, 0.217]	0.314, [0.313, 0.315]
	M23_tree	0.851, [0.850, 0.852]	0.410, [0.408, 0.412]	0.778, [0.773, 0.782]	0.779, [0.774, 0.783]	0.277, [0.275, 0.279]	0.362, [0.359, 0.365]
	Boogard_mlp	0.616, [0.615, 0.617]	0.145, [0.144, 0.156]	0.480, [0.475, 0.484]	0.710, [0.706, 0.714]	0.100, [0.100, 0.101]	0.206, [0.205, 0.207]
	Wassenaar_mlp	0.608, [0.607, 0.609]	0.137, [0.136, 0.138]	0.445, [0.439, 0.451]	0.730, [0.724, 0.735]	0.097, [0.097, 0.098]	0.199, [0.198, 0.199]
T123							
	M123_lr	0.778, [0.776, 0.779]	0.260, [0.258, 0.262]	0.689, [0.682, 0.697]	0.733, [0.725, 0.74]	0.176, [0.174, 0.178]	0.291, [0.288, 0.293]
	M123_mlp	0.820, [0.819, 0.821]	0.333, [0.331, 0.336]	0.749, [0.744, 0.754]	0.754, [0.749, 0.76]	0.227, [0.225, 0.229]	0.328, [0.326, 0.331]
	M123_tree	0.854, [0.853, 0.855]	0.418, [0.415, 0.421]	0.790, [0.784, 0.796]	0.772, [0.766, 0.778]	0.281, [0.278, 0.283]	0.360, [0.356, 0.363]
	Boogard_tree	0.616, [0.615, 0.617]	0.150, [0.149, 0.151]	0.450, [0.450, 0.450]	0.724, [0.724, 0.724]	0.098, [0.098, 0.098]	0.198, [0.198, 0.198]
	Wassenaar_mlp	0.608, [0.607, 0.609]	0.134, [0.133, 0.135]	0.438, [0.432, 0.444]	0.737, [0.731, 0.743]	0.098, [0.098, 0.098]	0.200, [0.199, 0.201]

Figure 3 summarizes the POD prediction performance of models on the test set according to the AUROC and AUPRC metrics. The upper two graphs display MLP and tree-based model performances across all time phase combinations (T1-T123). Performance was highest for models M3, M23 and M123 taking postoperative data (T3) into account. Models M12–M123 incorporating data from multiple time phases

seemed to perform better than models M1–M2 focusing on one single phase. Except for the combined pre- and intraoperative phase (T12), tree-based models outperformed MLPs. Tree-based model M123 ingesting all perioperative data (T123) showed highest AUROC as well as AUPRC metrics (see Figure 3).

Prediction performance of MLP, LR, tree, and baseline models – adopted from Wassenaar et al. and Boogaard et al. – applied to pre- and intraoperative data (T12), are shown in the two lower graphs of Figure 3. The proposed MLP model was superior to the linear LR model as well as the retrained or applied reference models. The best reference model for T12 was the retrained MLP model based on Boogard et al. (see Figure 3). Extended Figure 2 and Extended Figure 3 – included in Appendix2 – display AUROC and AUPRC graphs for all model variants, baselines, and time phase combinations.

Table 5 summarizes further evaluation metrics for models per time phase combination (T1-T123) evaluated on the bootstrapped test set. The best baseline models (for Wassenaar or Boogaard) are presented as well. Non-linear tree-based models outperformed linear LR across all time phase combinations (T1-T123). Tree-based models showed higher evaluation metrics than MLP models except for one time phase (T12) (see Table 8). Non-linear MLPs outperformed linear LR with respect to the AUPRC metric for all time phases (T1-T123). Both non-linear models variants – MLPs and trees – clearly outperformed baseline models.

The best performing non-linear tree-based model variant M123 was trained on all perioperative data (T123). This model showed a mean AUROC of 0.854 (95% CI [0.853, 0.855]) and a mean AUPRC of 0.418(95% CI [0.415, 0.421]]). Model variant M12, which incorporated data from the preoperative- (T1) and intraoperative (T2) phase omitting postoperative data (T3), yielded a mean AUROC of 0.777 (95% CI [0.776, 0.778]), a mean AUPRC of 0.269 (95% CI [0.268, 0.271]). Extended Table 9 in Appendix 1 shows metrics achieved on the training dataset without a tendency of under- or overfitting.

Discussion

Principal Results

Our results show that non-linear models can better predict POD onset in the recovery room than linear LR models especially when ingesting features from multiple perioperative phases. Tree-based models outperformed MLP models in time phases T1-T123 except for T2. This observation could be explained by the selected feature set that was different for MLPs determined via cross-validation on the training data (see Extended Table 4 and Extended Table 5 in Appendix 1). Retrained and applied baseline models by Wassenaar and Boogaard – originally developed as delirium prediction models for the intensive care admission – yielded moderate performance in the recovery room setting.

Although most of the univariate significant variables – like ASA score – are already known from clinical studies [54-57], it could be shown that additional parameters like intraoperative EEG edge frequencies and procedure durations were discriminative as well. Results must be interpreted carefully since no cohort matching – e.g., for reducing cofounding bias in a case-control study – was done.

Clinical Relevance

In clinical practice, it is desirable to know the risk for POD at the end of the intraoperative phase. This knowledge could be used to initiate preventive measures such as transportation to a noise-reduced ward after the surgery [8, 26, 27]. Models ingesting T12 make predictions before the admission to a recovery room. Thus, the physician can decide to transfer the patient to a specialized ward.

Assuming 100 surgeries per day through all three hospital sites including 10 real cases of POD. The application of the MLP M12 with a fixed sensitivity at 0.80 and a corresponding precision of 0.20 would lead to 8 correct transfers – of patients really suffering from POD – and 32 incorrect transfers – of patients not suffering from POD – to a specialized ward after surgical procedures. With a usual ICU size of 15-20 patients, the results highlight that a low precision is a main impediment for implementing trained models in a real clinical setting.

Comparison with Related Work

Original work by Wassenaar et al. and Boogard at al. focused on delirium prediction based on data available early after admission [18-20]. We could achieve a maximum AUROC of 0.61 using preoperative data by retraining their models, which seems to be complementary to external validation studies [21]. In our setup, the highest observed AUROC achieved for this time phase was 0.715. Xue et al. combined pre- and intraoperative data for training a MLP, reporting an AUROC of 0.715 and an AUPRC of 0.731 on data with 52.6% prevalence [22]. MLP model M12, which was also trained on pre- and intraoperative data, achieved a similar mean AUROC value (0.777). Due to the reduced prevalence, the mean AUPRC was noticeably lower (0.269). Low POD prevalence was explicitly addressed by Davoudi et al. using oversampling [6], we wanted to train an applicable model without changing the prevalence. Davoudi et al. and Bishara et al. achieved promising AUROC values over 0.80 with non-linear models on preoperative data, but did not report any AUPRC metrics [6, 24]. This would have been beneficial for a comprehensive comparison. Racine et al. compared a linear LR with a MLP approach. Their MLP model achieved an AUROC of 0.71 and a linear LR model achieved an AUROC of 0.69 [23]. Most related work investigating the application of machine learning for POD prediction with linear LR during a clinical trial incorporating few samples and specialized attributes [13-17]. Scores explicitly designed for assessing cognitive impairments – like the Mini-Mental State Examination (MMSE) – are highly correlated with delirium and were included in these studies as predictor variables [23, 14]. Positive ICD or CAM values during hospitalization were used by referenced work for the target definition [20-24]. To our knowledge, no previous study focused on a Nu-

DESC POD assessment in a recovery room setting. Our models are openly accessible and can be evaluated in other medical centers.

Limitations

Due to the vast amount of records, there was no chance of ensuring clinical correctness for all extracted EHRs. The feature selection process based on univariate test statistics moreover ignored dependencies between covariates, which may have been beneficial for the predictive performance [58]. Some features also showed high predictive power but low availability. We did not use feature interpretation methods – such as LIME or SHAP – as such methods are themselves poorly understood and may lead to wrong conclusions about model and data [58, 59]. Since we conducted a single-center study, results could have benefited from external validation.

Models incorporating T3 provide a POD assessment without relying on the actual observed Nu-DESC. Results were displayed to assess the relevance of covariates measured into the recovery room. We focused our clinical interpretation solely on MLP model M12 ingesting data up to T2. Cases with later POD onsets in ICUs or cases bypassing the recovery room were ignored but can be investigated in further studies. A prospective study that validates the predictions of our models also focusing on a clinical assessment regarding the Nu-DESC would be beneficial towards a clinical application.

Conclusion

This study demonstrates that machine learning can be used to predict POD assessed by the Nu-DESC in the recovery room, where the incorporation of different intraoperative phases as feature sets proved useful. Overall, non-linear models were superior to linear LR techniques as well as known published models. However, strategies for highly imbalanced data must be developed to implement solutions in clinical practice.

Contributions

NG extracted and preprocessed the EHR, trained and evaluated the machine learning models, and wrote the first paper draft. SB revised the code. SH, SB, and FB contributed to the methodological study design. MM, BW, FB, and CS contributed with clinical expertise. SP ensured statistical correctness. All authors read and approved the final manuscript.

Conflicts of Interest

None declared

Funding Source

Internal Funding

Abbreviations

AUC: Area under the curve
BP: Blood pressure
CAM: Confusion Assessment Method
CI: Confidence Interval
CRP: C-reactive protein
CV: Cross validation
EHR: Electronic health records
ESA: European Society of Anaesthesiology
ICU: Intensive Care Unit
IQCODE: Informant Questionnaire on Cognitive Decline in the Elderly
LIME: Local interpretable model-agnostic explanations
LR: Logistic regression
MAD: Median absolute deviation
MLP: Multi-layer perceptron
MMSE: Mini-Mental State Examination
MWU: Mann-Whitney U
Nu-DESC: Nursing Screening Delirium Scale
OR: Odds ratio
PCV: Pressure Control Ventilation
SEF: Spectral edge frequency
SHAPE: Shapley Additive exPlanations

References

1. Oh, S. T., & Park, J. Y. (2019). Postoperative delirium. Korean journal of anesthesiology, 72(1), 4
2. Sánchez, A., Thomas, C., Deeken, F., Wagner, S., Klöppel, S., Kentischer, F., ... & Rapp, M. A. (2019). Patient safety, cost-effectiveness, and quality of life: reduction of delirium risk and postoperative cognitive dysfunction after elective procedures in older adults—study protocol for a stepped-wedge cluster randomized trial (PAWEL Study). Trials, 20(1), 1-15.
3. Rudolph, J. L., & Marcantonio, E. R. (2011). Postoperative delirium: acute change with long-term implications. Anesthesia and analgesia, 112(5), 1202.
4. Saller, T., Hofmann-Kiefer, K. F., Saller, I., Zwissler, B., & von Dossow, V. (2021). Implementation of strategies to prevent and treat postoperative delirium in the post-anesthesia caring unit. Journal of clinical monitoring and computing, 35(3), 599-605.
5. Rudolph, J. L., Jones, R. N., Levkoff, S. E., Rockett, C., Inouye, S. K., Sellke, F. W., ... & Marcantonio, E. R. (2009). Derivation and validation of a preoperative prediction rule for delirium after cardiac surgery. Circulation, 119(2), 229-236.
6. Davoudi, A., Ozrazgat-Baslanti, T., Ebadi, A., Bursian, A. C., Bihorac, A., & Rashidi, P. (2017, October). Delirium prediction using machine learning models on predictive electronic health records data. In 2017 IEEE 17th

International Conference on Bioinformatics and Bioengineering (BIBE) (pp. 568-573). IEEE.

7. Radtke, F. M., Franck, M., Schust, S., Boehme, L., Pascher, A., Bail, H. J., ... & Spies, C. D. (2010). A comparison of three scores to screen for delirium on the surgical ward. World journal of surgery, 34(3), 487-494.
8. Aldecoa, C., Bettelli, G., Bilotta, F., Sanders, R. D., Audisio, R., Borozdina, A., ... & Spies, C. D. (2017). European Society of Anaesthesiology evidence-based and consensus-based guideline on postoperative delirium. European Journal of Anaesthesiology| EJA, 34(4), 192-214.
9. Grover, S., & Kate, N. (2012). Assessment scales for delirium: a review. World journal of psychiatry, 2(4), 58.
10. Neufeld, K. J., Leoutsakos, J. S., Sieber, F. E., Joshi, D., Wanamaker, B. L., Rios-Robles, J., & Needham, D. M. (2013). Evaluation of two delirium screening tools for detecting post-operative delirium in the elderly. British journal of anaesthesia, 111(4), 612-618.
11. Russell, M. D., Pinkerton, C., Sherman, K. A., Ebert, T. J., & Pagel, P. S. (2020). Predisposing and precipitating factors associated with postoperative delirium in patients undergoing cardiac surgery at a veterans affairs medical center: A pilot retrospective analysis. Journal of Cardiothoracic and vascular anesthesia, 34(8), 2103-2110.
12. Evered, L. A. (2017). Predicting delirium: are we there yet?. BJA: British Journal of Anaesthesia, 119(2), 281-283.
13. Moon, K. J., Jin, Y., Jin, T., & Lee, S. M. (2018). Development and validation of an automated delirium risk assessment system (Auto-DelRAS) implemented in the electronic health record system. International journal of nursing studies, 77, 46-53.
14. Chaiwat, O., Chanidnuan, M., Pancharoen, W., Vijitmala, K., Danpornprasert, P., Toadithep, P., & Thanakiattiwibun, C. (2019). Postoperative delirium in critically ill surgical patients: incidence, risk factors, and predictive scores. BMC anesthesiology, 19(1), 1-10.
15. Douglas, V. C., Hessler, C. S., Dhaliwal, G., Betjemann, J. P., Fukuda, K. A., Alameddine, L. R., ... & Josephson, S. A. (2013). The AWOL tool: derivation and validation of a delirium prediction rule. Journal of hospital medicine, 8(9), 493-499.
16. Kim, M. Y., Park, U. J., Kim, H. T., & Cho, W. H. (2016). DELirium prediction based on hospital information (Delphi) in general surgery patients. Medicine, 95(12).
17. Katznelson, R., Djaiani, G. N., Borger, M. A., Friedman, Z., Abbey, S. E., Fedorko, L., ... & Beattie, W. S. (2009). Preoperative use of statins is associated with reduced early delirium rates after cardiac surgery. The Journal of the American Society of Anesthesiologists, 110(1), 67-73.
18. Van den Boogaard, M., Pickkers, P., Slooter, A. J. C., Kuiper, M. A., Spronk, P. E., Van der Voort, P. H. J., ... & Schoonhoven, L. (2012). Development and

validation of PRE-DELIRIC (PREdiction of DELIRium in ICu patients) delirium prediction model for intensive care patients: observational multicentre study. Bmj, 344.

19. van den Boogaard, M. H. W. A., Schoonhoven, L., Maseda, E., Plowright, C., Jones, C., Luetz, A., ... & Pickkers, P. (2014). Recalibration of the delirium prediction model for ICU patients (PRE-DELIRIC): a multinational observational study. Intensive care medicine, 40(3), 361-369.
20. Wassenaar, A., van den Boogaard, M. H. W. A., van Achterberg, T., Slooter, A. J. C., Kuiper, M. A., Hoogendoorn, M. E., ... & Pickkers, P. (2015). Multinational development and validation of an early prediction model for delirium in ICU patients. Intensive care medicine, 41(6), 1048-1056.
21. Cowan, S. L., Preller, J., & Goudie, R. J. (2020). Evaluation of the E-PRE-DELIRIC prediction model for ICU delirium: a retrospective validation in a UK general ICU. Critical Care, 24(1), 1-3.
22. Xue, B., Li, D., Lu, C., King, C. R., Wildes, T., Avidan, M. S., ... & Abraham, J. (2021). Use of machine learning to develop and evaluate models using preoperative and intraoperative data to identify risks of postoperative complications. JAMA network open, 4(3), e212240-e212240.
23. Racine, A. M., Tommet, D., Madeline, L. D., Fong, T. G., Gou, Y., Tabloski, P. A., ... & Jones, R. N. (2021). Machine Learning to Develop and Internally Validate a Predictive Model for Post-operative Delirium in a Prospective, Observational Clinical Cohort Study of Older Surgical Patients. Journal of general internal medicine, 36(2), 265-273.
24. Bishara, A., Chiu, C., Whitlock, E. L., Douglas, V. C., Lee, S., Butte, A. J., ... & Donovan, A. L. (2022). Postoperative delirium prediction using machine learning models and preoperative electronic health record data. BMC anesthesiology, 22(1), 1-12.
25. Ruppert, M. M., Lipori, J., Patel, S., Ingersent, E., Cupka, J., Ozrazgat-Baslanti, T., ... & Bihorac, A. (2020). ICU Delirium-Prediction Models: A Systematic Review. Critical care explorations, 2(12).
26. van de Pol, I., van Iterson, M., & Maaskant, J. (2017). Effect of nocturnal sound reduction on the incidence of delirium in intensive care unit patients: an interrupted time series analysis. Intensive and Critical Care Nursing, 41, 18-25.
27. Xie, H., Kang, J., & Mills, G. H. (2009). Clinical review: The impact of noise on patients' sleep and the effectiveness of noise reduction strategies in intensive care units. Critical Care, 13(2), 1-8.
28. Oh, Y. S., Kim, D. W., Chun, H. J., & Yi, H. J. (2008). Incidence and risk factors of acute postoperative delirium in geriatric neurosurgical patients. Journal of Korean Neurosurgical Society, 43(3), 143.
29. Lehne, M., Sass, J., Essenwanger, A., Schepers, J., & Thun, S. (2019). Why digital medicine depends on interoperability. NPJ digital medicine, 2(1), 1-5.

30. Sittig, D. F., Wright, A., Osheroff, J. A., Middleton, B., Teich, J. M., Ash, J. S., ... & Bates, D. W. (2008). Grand challenges in clinical decision support. Journal of biomedical informatics, 41(2), 387-392.
31. Mann, H. B., & Whitney, D. R. (1947). On a test of whether one of two random variables is stochastically larger than the other. The annals of mathematical statistics, 50-60.
32. Benjamini, Y. (2010). Discovering the false discovery rate. Journal of the Royal Statistical Society: series B (statistical methodology), 72(4), 405-416.
33. Hanley, J. A., & McNeil, B. J. (1982). The meaning and use of the area under a receiver operating characteristic (ROC) curve. Radiology, 143(1), 29-36.
34. Szumilas, M. (2010). Explaining odds ratios. Journal of the Canadian academy of child and adolescent psychiatry, 19(3), 227.
35. Stone, M. (1974). Journal of the royal statistical society. Series B (Methodological), 36(2), 111-147.
36. Mohamad, I. B., & Usman, D. (2013). Standardization and its effects on K-means clustering algorithm. Research Journal of Applied Sciences, Engineering and Technology, 6(17), 3299-3303.
37. Gardner, M. W., & Dorling, S. R. (1998). Artificial neural networks (the multilayer perceptron)—a review of applications in the atmospheric sciences. Atmospheric environment, 32(14-15), 2627-2636.
38. Hornik, K., Stinchcombe, M., & White, H. (1989). Multilayer feedforward networks are universal approximators. Neural networks, 2(5), 359-366.
39. Hopfield, J. J. (1988). Artificial neural networks. IEEE Circuits and Devices Magazine, 4(5), 3-10.
40. Shekar, B. H., & Dagnew, G. (2019, February). Grid search-based hyperparameter tuning and classification of microarray cancer data. In 2019 second international conference on advanced computational and communication paradigms (ICACCP) (pp. 1-8). IEEE.
41. Bergstra, J., & Bengio, Y. (2012). Random search for hyper-parameter optimization. Journal of machine learning research, 13(2).
42. Lin, T. Y., Goyal, P., Girshick, R., He, K., & Dollár, P. (2017). Focal loss for dense object detection. In Proceedings of the IEEE international conference on computer vision (pp. 2980-2988).
43. Aurelio, Y. S., de Almeida, G. M., de Castro, C. L., & Braga, A. P. (2019). Learning from imbalanced data sets with weighted cross-entropy function. Neural processing letters, 50(2), 1937-1949.
44. Park, M. Y., & Hastie, T. (2007). L1-regularization path algorithm for generalized linear models. Journal of the Royal Statistical Society: Series B (Statistical Methodology), 69(4), 659-677.
45. Ho, T. K. (1995, August). Random decision forests. In Proceedings of 3rd international conference on document analysis and recognition (Vol. 1, pp. 278-282). IEEE.

46. Chen, T., & Guestrin, C. (2016, August). Xgboost: A scalable tree boosting system. In Proceedings of the 22nd acm sigkdd international conference on knowledge discovery and data mining (pp. 785-794).
47. Bradley, A. P. (1997). The use of the area under the ROC curve in the evaluation of machine learning algorithms. Pattern recognition, 30(7), 1145-1159.
48. Davis, J., & Goadrich, M. (2006, June). The relationship between Precision-Recall and ROC curves. In Proceedings of the 23rd international conference on Machine learning (pp. 233-240).
49. Wardhani, N. W. S., Rochayani, M. Y., Iriany, A., Sulistyono, A. D., & Lestantyo, P. (2019, October). Cross-validation metrics for evaluating classification performance on imbalanced data. In 2019 international conference on computer, control, informatics and its applications (ic3ina) (pp. 14-18). IEEE.
50. Yacouby, R., & Axman, D. (2020, November). Probabilistic extension of precision, recall, and f1 score for more thorough evaluation of classification models. In Proceedings of the First Workshop on Evaluation and Comparison of NLP Systems (pp. 79-91).
51. Efron, B., & Tibshirani, R. J. (1993). An introduction to the bootstrap. 57 Boca Raton.
52. www.github.com/ngiesa/icdep (accessed 14th of October 2023)
53. Collins, G. S., Dhiman, P., Navarro, C. L. A., Ma, J., Hooft, L., Reitsma, J. B., ... & Moons, K. G. (2021). Protocol for development of a reporting guideline (TRIPOD-AI) and risk of bias tool (PROBAST-AI) for diagnostic and prognostic prediction model studies based on artificial intelligence. BMJ open, 11(7), e048008.
54. Fineberg, S. J., Nandyala, S. V., Marquez-Lara, A., Oglesby, M., Patel, A. A., & Singh, K. (2013). Incidence and risk factors for postoperative delirium after lumbar spine surgery. Spine, 38(20), 1790-1796.
55. Afonso, A., Scurlock, C., Reich, D., Raikhelkar, J., Hossain, S., Bodian, C., ... & Flynn, B. (2010, September). Predictive model for postoperative delirium in cardiac surgical patients. In Seminars in cardiothoracic and vascular anesthesia (Vol. 14, No. 3, pp. 212-217). Sage CA: Los Angeles, CA: SAGE Publications.
56. Iamaroon, A., Wongviriyawong, T., Sura-Arunsumrit, P., Wiwatnodom, N., Rewuri, N., & Chaiwat, O. (2020). Incidence of and risk factors for postoperative delirium in older adult patients undergoing noncardiac surgery: a prospective study. BMC geriatrics, 20(1), 40.
57. de la Varga-Martínez, O., Gómez-Pesquera, E., Muñoz-Moreno, M. F., Marcos-Vidal, J. M., López-Gómez, A., Rodenas-Gómez, F., ... & Gómez-Sánchez, E. (2021). Development and validation of a delirium risk prediction preoperative model for cardiac surgery patients (DELIPRECAS): An observational multicentre study. Journal of Clinical Anesthesia, 69, 110158

58. Haufe, S., Meinecke, F., Görgen, K., Dähne, S., Haynes, J. D., Blankertz, B., & Bießmann, F. (2014). On the interpretation of weight vectors of linear models in multivariate neuroimaging. Neuroimage, 87, 96-110.
59. Wilming, R., Budding, C., Müller, K. R., & Haufe, S. (2022). Scrutinizing XAI using linear ground-truth data with suppressor variables. Machine learning, 1-21.